Physics of Plasmas ARTICLE scitation.org/journal/php

Microsecond timescale combustion of aluminum initiated by an underwater electrical wire explosion

Cite as: Phys. Plasmas **26**, 053510 (2019); doi: 10.1063/1.5096638
Submitted: 19 March 2019 · Accepted: 5 May 2019 ·
Published Online: 29 May 2019

View Online Export Citation CrossMark

A. Rososhek, S. Efimov, A. Goldman, S. V. Tewari, and Ya. E. Krasik

AFFILIATIONS

Physics Department, Technion, Haifa 32000, Israel

ABSTRACT

We report a direct observation of the microsecond time scale combustion of aluminum realized in underdamped electrical explosions of aluminum wires in the water environment. Experiments were conducted using a pulse power generator delivering a $\leq$200 kA current amplitude within an $\sim$1 μs rise-time. Time-resolved spectroscopy was applied to obtain the spectrum of AlO oxide absorption bands, and the temperature of oxides was determined. The results show that decreasing the wire diameter and increasing the discharge current density allow one to decrease the time delay in the appearance of AlO absorption bands to $\leq$1 μs with respect to the beginning of the wire explosion and significantly increase the rate of aluminum combustion up to $\sim 1.3 \times 10^3$ g/s.

I. INTRODUCTION

Research on aluminum (Al) combustion has attracted enduring attention because of the large enthalpy of the exothermic reaction realized as a result of its combustion with surrounding oxidizers (H_2O, CO_2, CO, NO, NO_2, and O_2). Because of the positive enthalpy of this reaction, Al powders have been utilized for many years as an additional energy source for propellants.[1] In the case of Al combustion in water, one can obtain[2] up to $\sim$60 kJ/g of the energy released in the reaction $2Al(s) + 3H_2O(l) = Al_2O_3(s) + 3H_2(g)$. The ignition temperature of this reaction is $\sim$1000 K,[3] and the required energy density deposition ranging from 2.6 to 5 kJ/g was found to depend considerably on the experimental conditions.[4–8]

During the last 60 years, Al combustion in different environmental conditions was studied experimentally, theoretically, and numerically. In Beckstead's comprehensive review,[9] experimental data for Al combustion are provided and summarized, and the results of different models are compared. In some of the models, the ignition of Al combustion is considered to start only when the oxide shell is melted,[1] whereas the authors of other models speculated that this process starts with the failure of the oxide shell integrity.[6] The Al combustion numerical modeling considers several stages, which include the formation of Al sub-oxides forming Al oxide via surface and gas-phase reactions. However, reliable kinetic data for Al–H_2O reactions are available only for a rather narrow range of temperatures.[10]

Earlier experimental research[9] showed that the typical burning time, τ_b, of micron-size Al particles is in the millisecond time scale. By combining a variety of experimental data for burning time vs Al particle diameter D_0 at different pressures and temperatures, Beckstead[9] obtained semi-empirical dependence $\tau_b[\text{ms}] = 0.003 D_0^{1.99}[\mu\text{m}]$. This relation agrees with the analytically obtained law, $\tau_b = D_0^2/\beta$, where $\beta = 64 \times [d(D^2)/dt]$.[11] Thus, $\tau_b \leq 10^{-4}$ s can be expected for particles of $D \leq 10$ μm. It was shown that the value of τ_b depends significantly on the pressure, temperature, and oxygen concentration realized in the combustion of Al particles in different experiments.[4] Taking these parameters into account, a more general semi-empirical expression was suggested:[9] $\tau_b = 0.0123 D_0^{1.8}/CP^{0.1}T_0^{0.2}$, where C is the concentration of water, P [atm] is the pressure, and T_0 [K] is the temperature required for beginning the Al combustion. This temperature is significantly (2–3 times) smaller than the aluminum oxide melting temperature of 2300 °C.[12] Yet, let us note that these investigations were performed at $P \leq 5 \times 10^6$ Pa and $T \leq 3$ kK.

In our recent experimental studies of underwater electrical explosions of Al wires[13] and Al wire arrays[14–17] conducted in 10^{-7}–10^{-6} s timescales, a significantly brighter light emission and larger energy transference to the water flow were obtained than in copper wire explosions. To explain these observations, the possibility of Al wire combustion was suggested. The process of underwater electrical wire explosion is characterized by the formation of an extreme state of the material. For instance, energy density deposition is in the range of 10–100 kJ/g, the temperature reaches several eV, and the pressure approaches 10^{10} Pa. These conditions differ drastically from that of previous combustion studies. Here let us note that in earlier research[18]

on Al wire explosion in water in a time scale of several tens of microseconds, the effect of Al combustion on generated shock wave was not obtained. However, spectroscopic research[19] on the light emission of AlO and OH oxide bands during intense millisecond time scale heating of Al wire showed evidence of the Al combustion process.

In this paper, we present experimental data for Al combustion ignited by an underwater electrical explosion of a single Al wire and Al wire arrays in the microsecond time scale. Time- and space-resolved streak images of the wires' light emission and the time-resolved spectrum of AlO oxide absorption bands showed evidence of Al combustion, which is realized when the wire explosion is characterized by underdamped electrical discharge. This spectrum appears to be due to AlO oxide light absorption, which occurs as a result of gas-phase combustion of Al in the presence of surrounding water oxidizers.[20,21] AlO spectroscopy is frequently used to identify species in Al combustion,[22–24] and to detect whether the Al is burning.[25–28] Moreover, by using the high-resolution spectra of the AlO B-X transition, AlO vibrational temperatures can be determined.[20,21,29–36] These findings suggest that the presence of AlO serves as clear evidence of an Al combustion process on a microsecond time scale.

II. EXPERIMENTAL SETUP AND DIAGNOSTICS

The experimental setup is shown in Fig. 1. The experiments were conducted using a microsecond-time scale pulse generator (see Ref. 7) with a stored energy of ∼3.1 kJ at a charging voltage of 25 kV, resulting in a current amplitude of ∼280 kA with a rise time of ∼1.25 μs. The total discharge circuit inductance was ∼70 nH with short circuit load having inductance of ∼15 nH. A 45 mm long Al wire (150 μm, 250 μm, 500 μm, or 800 μm in diameter) was placed coaxially inside the chamber filled with de-ionized water between the high voltage and grounded electrodes. Hereinafter, the terms Al 150, Al 250, Al 500, and Al 800 are used to refer to Al wires having a diameter of 150 μm, 250 μm, 500 μm, and 800 μm, respectively. In addition to single wire explosions, we conducted experiments with planar Al wire array explosions. In these experiments, wire arrays having 50 wires 50 μm in diameter and 10 wires 152 μm in diameter (hereafter, a 50 × 50 wire array and 10 × 152 wire array) were used.

The discharge current was measured using a self-integrated Rogowski coil and the total voltage drop along the wire was measured using a Tektronix voltage divider connected to the high voltage electrode. A 532 nm CW laser EN60825–1:2007 (see Fig. 1) was used for optical alignment prior to the generator shots. The time- and space-dependent evolution of exploding wire self-emission in the visible range of light was obtained using an Optronis SC-10 streak camera with neutral filters placed at the front of the camera input slit. To obtain a spectrum of the light emission of the exploding wire, an imaging spectrometer Chromex 250 having three different gratings with a streak camera at its output was used. With a 300 grooves/mm grating, this optical setup was used to obtain spectra of the AlO oxide bands in the broad wavelength range 411 nm–646 nm with a spectral resolution of ∼0.71 Å/pix. To observe bands of OH radicals, a grating with 1800 grooves/mm grating was used, which covers 300.94–316.68 range with a spectral resolution of 0.15 Å/pix. The time resolution was ∼360 ns/pix for a streak timebase of 500 μs, 150 ns/pix for a streak timebase of 200 μs, and 36 ns/pix for a streak timebase of 50 μs. To synchronize the operation of the high-current generator and the streak camera, a Stanford Digital Delay Generator DG645 was used.

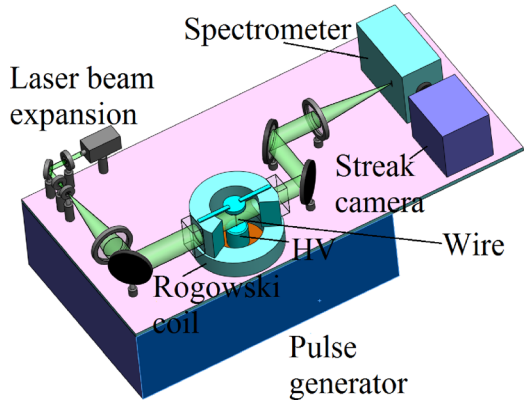

FIG. 1. Experimental setup.

III. EXPERIMENTAL RESULTS

In Figs. 2–4, one can see typical waveforms of the discharge current and resistive voltage at different timescales, together with the deposited power/energy for Al 800 and Al 500 wire and 50 × 50 wire array explosions. One can see that explosions of Al 800 wire are characterized by an almost critically damped discharge with a current density of $\lesssim$31 MA/cm^2, which agrees well with the specific current action for Al, $h \approx 6 \times 10^8$ A^2 s/cm^4.[37] Here, the maximal current density was calculated by assuming uniform current density radial distribution in the wire's cross section, which was estimated using the streak images of the expanding wire. The total energy deposited into the Al 800 wire until the first zero of the discharge current was ∼2.8 kJ, which corresponds to a deposited energy density of ∼45 kJ/g. The total average resistance of the discharge channel at the end of the energy deposition ($\tau_d \sim 2.4$ μs with respect to the beginning of the discharge current) reaches ∼0.3 Ω, which implies the formation of a low-ionized highly resistive plasma channel.

In the case of Al 500 wire explosions, the discharge was underdamped, that is, after a fast decrease in the discharge current, a re-strike with a fast decaying oscillating current was obtained. The maximal resistance of the discharge channel did not exceed ∼0.5 Ω at $\tau_d \sim 0.9$ μs. The total energy deposited into the Al wire was ∼2.7 kJ, which is slightly lower than that observed for the Al 800 explosion, but the time of the energy deposition was considerably longer, ∼2.2 μs. Furthermore, the maxima of current density and energy density deposition were different, 22 MA/cm^2 and ∼115 kJ/g, as compared with the results for Al 800 wire explosions.

An explosion of a 50 × 50 wire array is qualitatively similar to that of an Al 500 wire. However, the discharge current re-strike amplitude was almost two times the first maximum of the discharge current when the explosion occurred. Indeed, the explosion time was considerably earlier at $\tau_d \approx 500$ ns with a maximal resistance of the discharge channel of ∼0.9 Ω. Assuming uniform distribution of the current between the wires, one obtains a current density of almost ∼49 MA/cm^2 near the explosion time and ∼1.3 MA/cm^2 at the re-strike maximum. The total energy deposited into the wire was ∼2.4 kJ, energy density deposition ∼200 kJ/g or ∼56 eV/atom, and the energy deposition time reached ∼2.5 μs. However, it should be noted that when the wire's diameter is sufficiently small, it might act as an initiating wire[38]

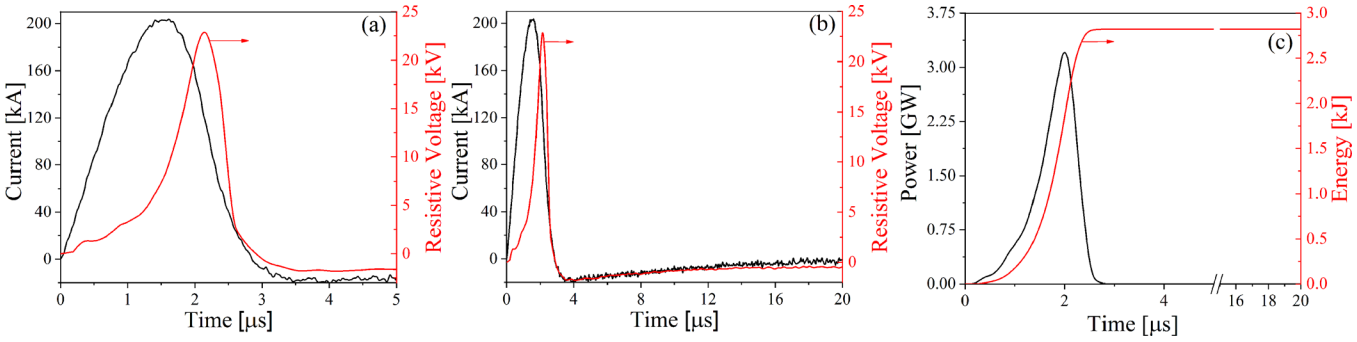

FIG. 2. Typical waveforms of the discharge current and resistive voltage [(a) and (b)] at different timescales together with deposited power and energy (c) for an Al 800 wire explosion.

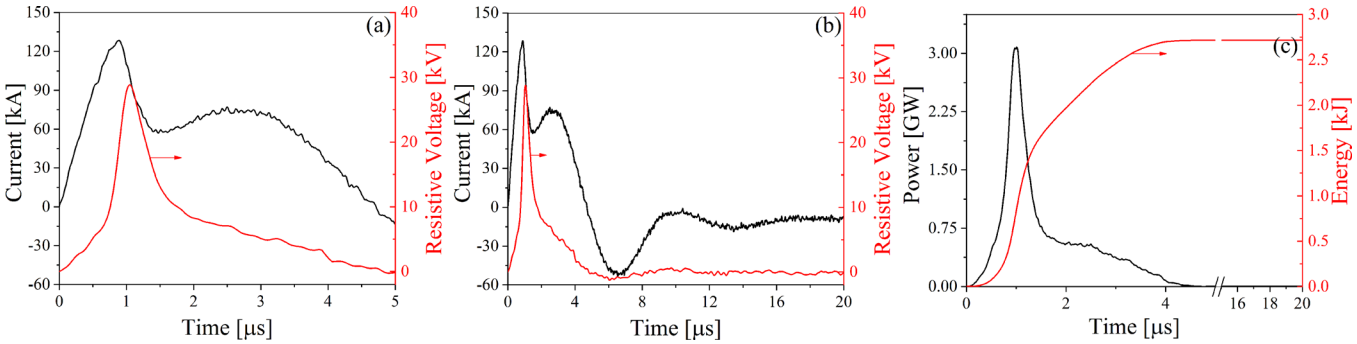

FIG. 3. Typical waveforms of the discharge current and resistive voltage [(a) and (b)] at different timescales together with deposited power and energy (c) for an Al 500 wire explosion.

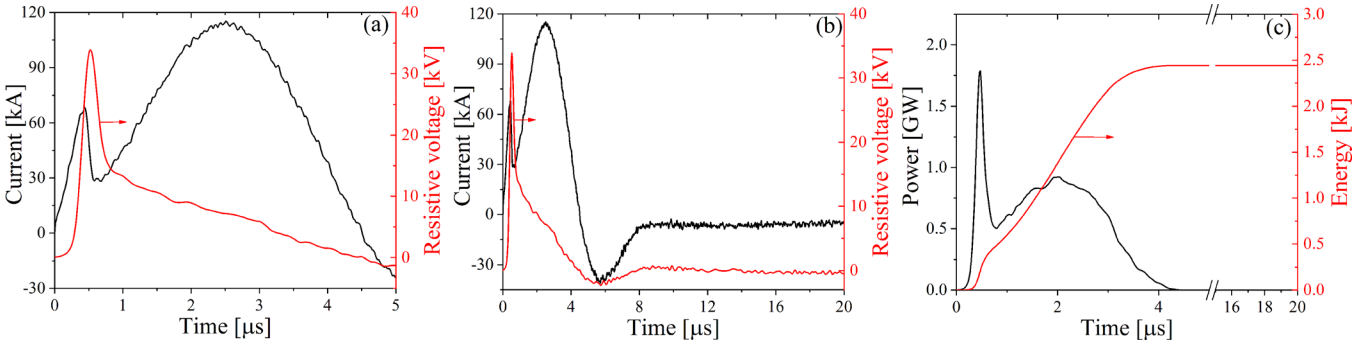

FIG. 4. Typical waveforms of the discharge current and resistive voltage [(a) and (b)] at different timescales together with deposited power and energy (c) for a 50 × 50 μm wire array explosion.

such that the discharge current redistributes between the wires and plasma formed in water surrounding these thin wires.

The spatial and temporal distributions of light emitted by exploding Al wires are shown in Fig. 5. All wire explosions show a qualitatively identical initial increase in light intensity similar to that registered in earlier experiments.[13] It has been suggested that this microsecond time scale increase in light intensity is related to the emission of sub-micron size particles during the discharge channel expansion.[39] This implies sufficiently low plasma density for the photon mean free path to become sufficiently large and result in light emission from the entire volume of the discharge channel instead of from only the channel surface.

In Fig. 5, streak images of exploding Al 800, Al 500, Al 250, and Al 150 wires' self-light emission with a streak timebase of 500 μs are shown. In this figure, it is seen that the termination of the light emission first occurs at the wire periphery and later at the wire axis. This can be explained by the rapidly decreasing density of the expanding discharge plasma channel and its mixing with the surrounding

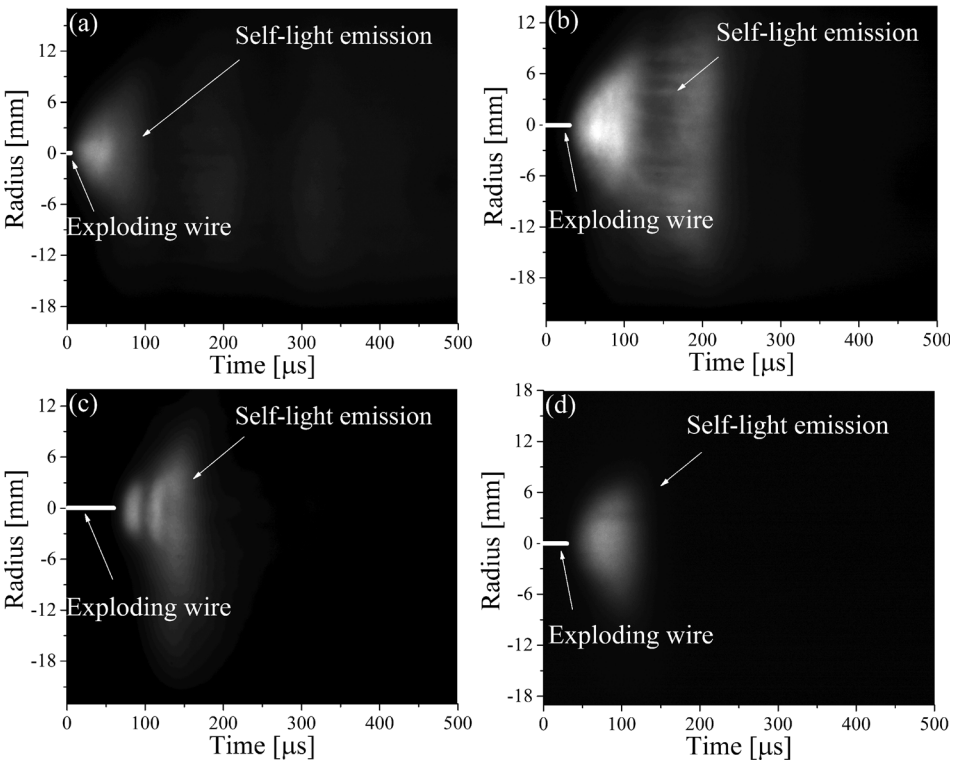

FIG. 5. Streak images of Al 800 (a), Al 500 (b), Al 250 (c), and Al 150 (d) wire explosions.

water/vapor medium, leading to fast cooling of the plasma. One can assume that at earlier times of the light emission evolution, the shape of the light intensity pattern seen in Fig. 5 roughly corresponds to the discharge channel width. Therefore, taking as an example an Al 500 explosion [see Fig. 5(b)], for the time $t \approx 75$ μs, the radius of the wire can be estimated as ~11 mm. The latter corresponds to an $\sim 10^3$ times decrease in the wire's density, which becomes significantly smaller than that of the surrounding water. Thus, considering that at $\tau_d > 75$ μs the temperature of the discharge channel is $\leq 10^4$ K, one can suppose that the pressure in the channel also becomes smaller than that of water, leading to an intense mixing and cooling process of the plasma.

Another qualitative observation is that the temporal evolution of light emission of Al 500 and Al 250 [see Figs. 5(b) and 5(c)] explosions is not uniform, in contrast to that of Al 150 explosions; that is, one obtains two light intensity maxima with a time interval of ~120 μs and ~30 μs for Al 500 and Al 250 explosions, respectively. The time evolution of the light intensity (in arbitrary units) at the axis ($r = 0$) in Al 150, Al 250, Al 500, and Al 800 explosions is shown in Fig. 6, and the main parameters of these dependencies are summarized in Table I. One can see that, for an Al 800 explosion, the only one maximum of the light intensity is obtained at $\tau_d \sim 30$ μs, which has an ~20 μs plateau followed by an ~20 μs decrease in light intensity. In contrast, the light emission obtained in the case of Al 500 explosions is characterized by two maxima, at $\tau_d \sim 50$ μs and $155 \leq \tau_d \leq 180$ μs, and the intensity of the first maximum is ~2 times more intense than that of the Al 800 explosion. Similarly, the Al 250 explosion shows two maxima in light intensity with a shorter time interval, whereas the Al 150 explosion shows only one, suggesting the possibility that the

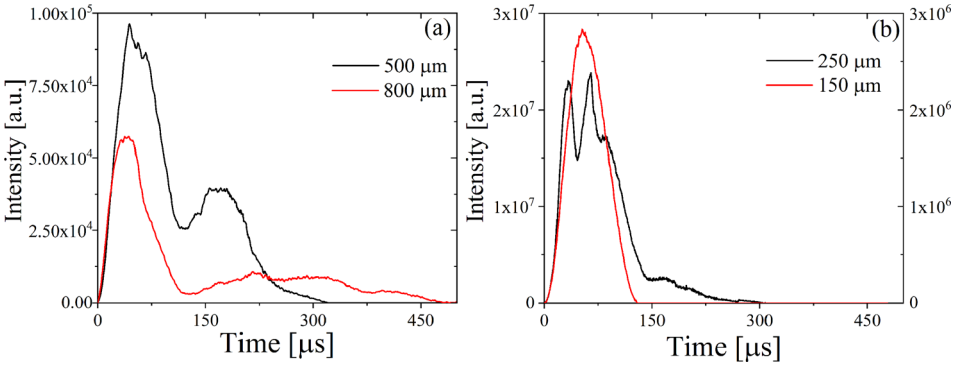

FIG. 6. Time evolution of the light intensity measured at the wire axis obtained in the explosion of single Al wires with different diameters.

TABLE I. Main parameters of light emission by the exploded wires.

Diameter [μm]	Time of the first intensity maximum [μs]	Intensity at the 1st maximum [a.u.]	Time of the second intensity maximum [μs]	Intensity at the 2nd maximum [a.u.]
150	~53	~3 000	n/a	n/a
250	~33	~23 000	~65	~24 400
500	~44	~96	155–180	~40
800	31–50	~65	n/a	n/a

combustion is faster. The second maximum of the light intensity emission obtained for Al 500 and Al 250 explosions cannot be related to plasma heating by the discharge current, which was terminated long before, or to the discharge channel pulsation, which should be seen in the streak image. Thus, one can suppose that the second maximum of the light intensity is related to the evolution of the Al combustion process, which depends on the wire's initial radius and energy density deposition. In addition, one can see that the intensity of the light emission in Al 250 and Al 150 explosions is more than ten times larger than that of Al 800 and Al 500 explosions, which can be related to intense combustion ignited by the Al 250 and Al 150 wires' explosion.

Direct evidence of Al combustion was obtained when time-resolved spectroscopy was applied. First, let us note that measurements of the time-dependent spectrum performed with Al 800 explosion wires did not show resolvable AlO oxide spectral bands. Only a very weak continuous light spectrum was registered during ~75 μs with respect to the beginning of the discharge current. However, very clear and qualitatively similar time-dependent AlO oxide spectra were recorded in the case of Al 500, Al 250, and Al 150 wire explosions and 10×152 and 50×50 wire array explosions. Namely, the observed spectra consist of AlO absorption bands and the Planck-like radiation emitted by the plasma channel. Absorption lines corresponding to AlO $X^2\sum^+ \rightarrow B^2\sum^+$ ($v' = -2 \cdots +2$ – $v' = -2 \cdots +2$) transitions were identified and assigned using data provided in the literature.[40] In an Al 500 wire explosion, these absorption spectral bands, related to AlO absorption, become resolvable from $\tau \geq 30$ μs with respect to the beginning of the discharge current [see Fig. 7(a)], and these band spectra become indistinguishable at $\tau \geq 300$ μs. An example of an AlO band spectrum containing the lines corresponding to transitions with different Δv (0, ±1) and averaged over ~14 μs is shown in Fig. 7(b). The spectral lines originating from different vibrational levels allow the average temperature to be estimated by using Boltzmann energy states population analysis. The determination of individual vibrational line intensity required for the temperature evaluation was performed using PGOPHER software[41] running with an AlO simulation input file.[42] Using vibrational line intensity derived from the vibrational band with $\Delta v = 0$, the temperature ~5200 ± 600 K was obtained. Let us note that this value of AlO oxides temperature coincides satisfactorily with the temperature of ~5700 K calculated from the Planck's radiation of the plasma channel. In the case of Al 250 and Al 150 wire explosions and 10×152 and 50×50 wire array explosions, this approach for the temperature estimation was not used because of a strong background light intensity which shades the vibrational line intensities. In these experiments, using continuous spectra and assuming blackbody radiation, the temperature is estimated as 10 000 ± 400 K, 12 500 ± 500 K, 7500 ± 300 K, and 13 500 ± 500 K for Al 150 wire, Al 250 wire, 10×152 array, and 50×50 array explosions, respectively. These temperatures are larger than that of Al 500 wire explosion, while the maximal temperature is obtained in the case of the smallest diameter 50×50 array explosions.

In Table II, a summary of explosion parameters is presented. One can see that for the case of 10×152 wire array having a total diameter of ~480 μm and, consequently, almost the same mass as Al 500 wire, the parameters of the explosion are very similar to those realized for Al 500 wire explosion. However, the temperature is ~1500 K higher for the former case which can be associated with more intense combustion process. This agrees with the shorter and stronger light emission obtained for the case of 10×152 wire array explosion. A qualitatively similar trend can be found comparing Al 250 wire and 50×50 wire array explosion showing ~1000 K larger temperature for 50×50 wire array explosion despite the larger energy density deposition rate for Al 250 wire explosion.

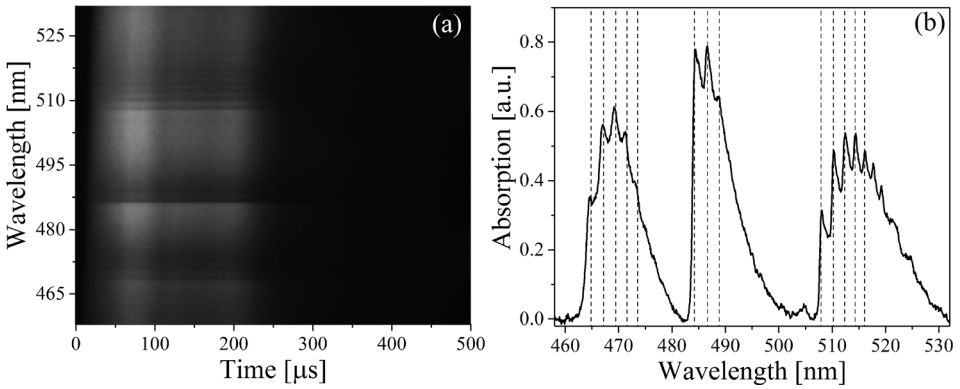

FIG. 7. (a) Streak image of the time-resolved spectrum; (b) absorption bands of AlO oxides corresponding to transitions with different Δv (0, ±1). Al 500 wire explosion.

TABLE II. Summary of explosion parameters.[a]

Explosion of	Maximal current density at the explosion [MA/cm^2]	Maximal current density at re-strike [MA/cm^2]	Deposited energy density [kJ/g]	Energy deposition time[b] [μs]	Energy density deposition rate [kJ/(g·μs)]
800 μm wire	31	n/a	45	1.1	41
500 μm wire	22	0.70	115	2.2	52
250 μm wire	35	0.95	465	3.2	145
150 μm wire	43	1.80	1160	2.4	483
10 × 152 μm wire array	43	1.0	135	2.2	61
50 × 50 μm wire array	49	1.30	200	2.5	80

[a]All the measured and calculated values have up to 10% experimental error.
[b]Time interval from 10% to 90% of the total energy deposited into the wire.

Now let us analyze the duration of the obtained AlO spectral bands. Similar to the streak images of self-emission intensity (see Fig. 6), the spectrally resolved images of AlO oxide bands showed a decrease in duration of these bands' absorption with the decrease in the wire diameter. Namely, whereas in Al 500 explosions the duration of resolvable band absorption was ∼300 μs, in Al 250 and Al 150 explosions these durations were ∼140 μs and ∼80 μs, respectively. In addition, the time delay between the beginning of the discharge current and the appearance of intense absorption of AlO bands decreased significantly with the decrease in the diameter of the Al wires, i.e., from ∼30 μs to ∼12 μs for Al 500 and Al 250 explosions, respectively. The fastest Al ignition was obtained in the case of electrical explosions of 10 × 152 and 50 × 50 wire arrays. Typical streak images of the spectra obtained in these explosions are shown in Fig. 8. One can see that the duration of the bands' absorption, as well as the time delay between the beginning of the discharge current and the appearance of band absorption, decreases further with the decrease in the wire diameter. Indeed, as one can see in a zoomed-in image of the spectrum obtained for a 50 × 50 wire array explosion [see Fig. 8(c)], this time delay becomes ≤1 μs.

The time evolution of normalized absorption intensities of the AlO oxide spectral line $\lambda = 486.1$ nm for Al 500 wire explosions and 10 × 152 μm and 50 × 50 μm wire array explosions are shown in Fig. 9. One can see that the decrease in the wire diameter while keeping approximately the same total mass of Al results in a significant acceleration of the combustion process. The main parameters of the Al combustion estimated using the AlO oxide absorption line are shown in Table III. Here, to estimate the Al mass burning rate we introduce the burning time of Al as the time duration of the AlO oxide absorption line intensity at its half maximum. One can see that the decrease in the wire diameter leads to a significant increase in the mass burning rate, reaching ∼1.33 mg/μs for 50 × 50 μm wire array explosion.

In addition, we conducted a few experiments with the explosion of Al 500 wire to obtain in the ultraviolet range 290–350 ns spectral bands (306.5 nm and 309.5 nm)[43] of OH radicals, which can be expected in the case of Al combustion. Indeed, in the range 306 nm–310 nm, rather strong absorption bands were obtained. However, in the same range, one can expect to obtain strong Al I (308.21 nm and 309.28 nm) and Al II (308.85 nm) spectral lines[44] which, because of Stark broadening, overlap these bands, thus complicating this spectral range analysis.

Finally, we attempted to obtain streak images of the H_α spectral line, which should allow the plasma density to be estimated. However, all our attempts, in which different spectral and time resolutions of the streak camera were used, failed. This can be related to the very fast formation of a plasma with a density $>10^{18}$ cm^{-3}, which, together with the van der Waals effect, lead to the significant broadening of this spectral line, making its intensity unresolvable on the intense continuous emission background.

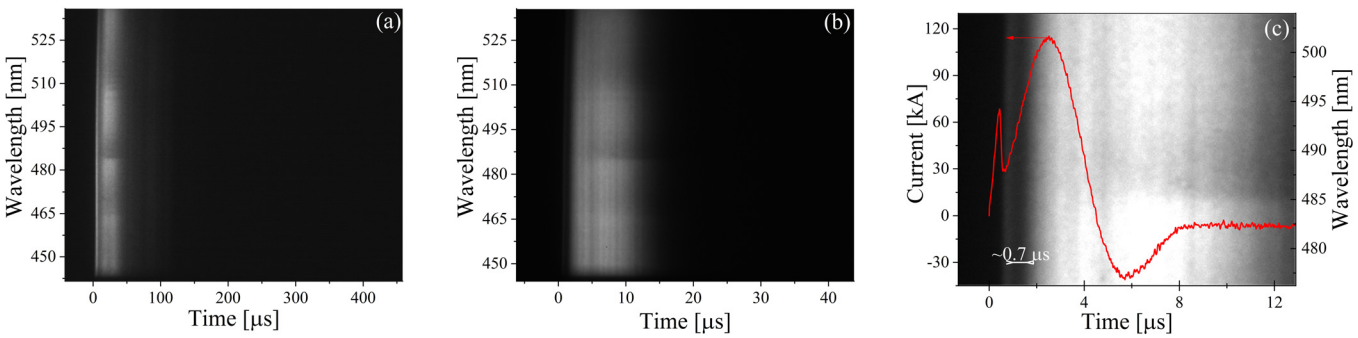

FIG. 8. Streak mages of the spectra obtained at the explosion of (a) 10 × 152 wire array and (b) 50 × 50 wire array; (c) enlarged streak image of the obtained spectrum for 50 × 50 wire array explosion overlapped with the discharge current waveform shown in red.

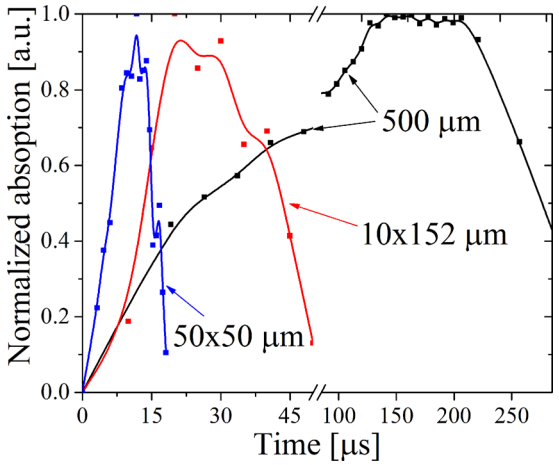

FIG. 9. Normalized absorption of $\lambda = 486.1$ nm line for Al 500 wire explosions (black), 10×152 μm (red), and 50×50 μm (blue) wire array explosions.

TABLE III. Main parameters of the Al combustion process.

Explosion type	Re-strike average current density amplitude [kA/cm^2]	Burning time [μs]	Mass of the aluminum [mg]	Mass burning rate [(g/s)$\times 10^3$]
500 μm	700 ± 70	251 ± 7	23.9	~0.09
10×152 μm	1000 ± 100	29.8 ± 0.7	22.0	~0.74
50×50 μm	1300 ± 130	8.9 ± 0.4	11.9	~1.33

IV. SUMMARY

Our experiments showed that an underwater electrical explosion of Al wire(s) provides sufficient conditions for efficient Al combustion on the microsecond time scale. Namely, phase transitions of exploding wire to the gas/plasma state, characterized by a temperature significantly exceeding 10^3 K and radial wire expansion, allow this Al gas/plasma to mix with water molecules, leading to a chemical combustion reaction, not only at the wire's surface but also in the bulk of the discharge channel.

The spectroscopic data, described in Sec. III, showed evidence of Al combustion realized within a time range $\leq 10^{-4}$ s and only when the explosion of the Al wire was characterized by underdamped fast decaying current discharge. For example, the Al 500 discharge with a current density up to 22 MA/cm^2, energy density deposition of ~115 kJ/g (~31 eV/atom), leads to the formation of low-resistivity ($\sim 4.4 \times 10^{-5}$ Ω·cm) highly ionized plasma consisting of neutral and singly ionized Al atoms with a temperature of several eV. Large pressure (~10^8 Pa) realized in the discharge channel[45,46] results in radial expansion with an average velocity of $\sim 1.5 \times 10^4$ cm/s, accompanied by a decrease in density and temperature. One can suppose that, because of the exploded wire's radiation and heat transfer, the water layer surrounding the wire can be vaporized, resulting in the formation of a layer of dense and relatively hot vapor with OH radicals. This vapor then mixes and reacts with Al atoms and ions, leading to the combustion reaction and formation of AlO oxide by the $Al + H_2O = AlO + H_2$ chemical reaction.

One can suppose that the absence of the AlO absorption spectrum in the case of an almost critically damped discharge of an Al 800 wire explosion can be related to the formation of a discharge channel consisting of liquid–vapor–low ionized plasma. The latter prevents efficient mixing and diffusion between the water vapors and the bulk of the channel material, and thus only the external layers of the exploded wire react with water. This qualitatively agrees with the significantly smaller light intensity and its fast decay in the case of Al 800 wire explosions as opposed to explosions of wires with smaller diameters, where light intensity gradually increased in time.

Wire array explosions show a promising approach for acceleration of aluminum combustion. The estimated burning time of aluminum (~9 μs) is several orders faster than that obtained in previous research studies.[9] It was found that the burning time depends on the discharge current re-strike amplitude. Furthermore, an analysis of light self-emission intensity evolution showed that the same mass of the wire material can pass the oxidization process almost eight times faster when a wire array is used instead of a single wire. Thus, by using an array with a large number of Al wires, each having diameter <10 μm, it may be possible to obtain significant additional input of the energy to the water flow, and thus achieve larger density, pressure, and temperature in the vicinity of implosion of converging either cylindrical or quasi-spherical shock waves.[16,46]

ACKNOWLEDGMENTS

This research was supported by the Israeli Science Foundation Grant No. 492/18 and in part by the Center for Absorption in Science, Ministry of Immigrant Absorption, State of Israel.

REFERENCES

[1] I. Glassman, American Rocket Society, ARS Preprint 938–59 (1959).
[2] J. D. Cox, D. D. Wagman, and V. A. Medvedev, CODATA Key Values Thermodyn. **1**, 19 (1984).
[3] O. J. Elgert and A. W. Brown, U.S. Atomic Energy Publication, IDO 16257 (1956).
[4] A. F. Belyaev, Yu. V. Frolov, and A. I. Korotkov, Combust., Explos. Shock Waves **4**, 182 (1968).
[5] A. G. Merzhanov, Yu. M. Grigorjev, and Yu. A. Gal'chenko, Combust. Flame **29**, 1 (1977).
[6] V. A. Ermakov, A. A. Razdobreev, A. I. Skorik, V. V. Pozdeev, and S. S. Smolyakov, Combust., Explos. Shock Waves **18**, 256 (1982).
[7] A. K. Lokenbakh, N. A. Zaporina, A. Z. Knipele, V. V. Strod, and L. K. Lepin, Combust., Explos. Shock Waves **21**, 69 (1985).
[8] V. M. Boiko, V. V. Lotov, and A. N. Papyrin, Combust., Explos. Shock Waves **25**, 193 (1989).
[9] M. W. Beckstead, *A Summary of Aluminum Combustion*, Brigham Young Univ Provo Ut, 2004.
[10] R. E. McClean, H. H. Nelson, and M. L. Campbell, J. Phys. Chem. **97**, 9763 (1993).
[11] G. A. E. Godsave, Symp. (Int.) Combust. **4**(1), 818–830 (1953).
[12] M. A. Gurevich and A. M. Stepanov, Fiz. Goreniya Vzryva **2**, 172 (1968) (in Russian).
[13] A. Grinenko, Ya. E. Krasik, S. Efimov, A. Fedotov, V. Tz. Gurovich, and V. I. Oreshkin, Phys. Plasmas **13**, 042701 (2006).
[14] S. Efimov, V. Tz. Gurovich, G. Bazalitski, A. Fedotov, and Ya. E. Krasik, J. Appl. Phys. **106**, 073308 (2009).
[15] L. Gilburd, S. Efimov, A. Fedotov-Gefen, V. Tz. Gurovich, G. Bazalitski, O. Antonov, and Ya. E. Krasik, Laser Part. Beams **30**, 215 (2012).

[16]O. Antonov, L. Gilburd, S. Efimov, G. Bazalitski, V. Tz. Gurovich, and Ya. E. Krasik, Phys. Plasmas **19**, 102702 (2012).
[17]A. Fedotov, D. Sheftman, V. Tz. Gurovich, S. Efimov, G. Bazilitski, V. I. Oreshkin, and Ya. E. Krasik, Phys. Plasmas **15**, 082704 (2008).
[18]W. M. Lee and R. D. Ford, J. Appl. Phys. **64**, 3851 (1988).
[19]M. R. Jones and M. Q. Brewster, J. Quant. Spectrosc. Radiat. Transfer **46**, 109 (1991).
[20]P. Bucher, R. A. Yetter, F. L. Dryer, T. P. Parr, and D. M. Hanson-Parr, Symp. (Int.) Combust., [Proc.] **27**, 2421–2429 (1998).
[21]M. Beckstead, Y. Liang, and K. Pudduppakkam, Combust., Explos. Shock Waves **41**, 622 (2005).
[22]P. Bucher, R. A. Yetter, F. L. Dryer, E. P. Viceni, T. P. Parr, and D. M. Hanson-Parr, in *Proceedings of 33rd JANNAF Combustion Subcommittee Meeting CPIA Publication 653* (1996), Vol. II, pp. 449–458.
[23]J. R. Carney, J. M. Lightstone, J. D. Koch, and S. R. Piecuch, in *Proceedings of 14th International Detonation Symposium* (2010), pp. 316–327.
[24]J. L. Gottfried, Technical Report No. ARL-MR-0736, Army Research Laboratory, 2010.
[25]T. A. Roberts, R. L. Burton, and H. Krier, Combust. Flame **92**, 125 (1993).
[26]Z. X. Yan, J. H. Wu, S. Ye, D. Hu, and X. D. Yang, J. Appl. Phys. **101**, 024905 (2007).
[27]V. Tanguay, S. Goroshin, A. J. Higgins, and F. Zhang, Combust. Sci. Technol. **181**, 670 (2009).
[28]J. R. Carney and J. M. Lightstone, in Proceedings of the 6th US National Combustion Meeting (2009).
[29]T. Bazyn, H. Krier, and N. Glumac, Proc. Combust. Inst. **31**, 2021–2028 (2007).
[30]J. M. Lightstone, J. R. Carney, C. J. Boswell, and J. Wilkinson, AIP Conf. Proc. **955**, 1255–1258 (2007).
[31]T. Bazyn, H. Krier, and N. Glumac, Combust. Flame **145**, 703 (2006).
[32]N. Glumac, J. Servaites, and H. Krier, Combust. Sci. Technol. **172**, 97 (2001).
[33]P. Bucher, R. A. Yetter, F. L. Dryer, T. P. Parr, D. M. Hanson-Parr, and E. P. Viceni, Symp. (Int.) Combust., [Proc.] **26**, 1899–1908 (1996).
[34]P. Bucher, R. A. Yetter, F. L. Dryer, T. P. Parr, and D. M. Hanson-Parr, in *Proceedings of 34th JANNAF Combustion Subcommittee Meeting* (1997), Vol. II, pp. 295–305.
[35]S. Goroshin, J. Mamen, A. Higgins, T. Bazyn, N. Glumac, and H. Krier, Proc. Combust. Inst. **31**(2), 2011–2019 (2007).
[36]N. I. Poletaev and A. V. Florko, Combust., Explos. Shock Waves **44**, 437 (2008).
[37]V. S. Sedoi, G. A. Mesyats, V. I. Oreshkin, V. V. Valevich, and L. I. Chemezova, IEEE Trans. Plasma Sci. **27**, 845 (1999).
[38]E. A. Martin, J. Appl. Phys. **31**, 255 (1960).
[39]G. S. Sarkisov, P. V. Sasorov, K. W. Struve, and D. H. McDaniel, J. Appl. Phys. **96**, 1674 (2004).
[40]R. W. Pearse and A. G. Gaydon, *The Identification of Molecular Spectra*, 3th ed. (John Wiley & sons, 1963).
[41]C. M. Western, *PGOPHER Version 9.1* (University of Bristol Research Data Repository, 2016).
[42]J. C. Gómez Martín, S. M. Daly, J. S. A. Brooke, and J. M. C. Plane, Chem. Phys. Lett. **675**, 56 (2017).
[43]C. de Izarra, J. Phys. D: Appl. Phys. **33**, 1697 (2000).
[44]A. Kramida, Yu. Ralchenko, J. Reader, and NIST ASD Team, NIST Atomic Spectra Database (2018).
[45]Ya. E. Krasik, A. Grinenko, A. Sayapin, S. Efimov, A. Fedotov, V. Z. Gurovich, and V. I. Oreshkin, IEEE Trans. Plasma Sci. **36**, 423 (2008).
[46]Ya. E. Krasik, A. Fedotov, D. Sheftman, S. Efimov, A. Sayapin, V. Tz. Gurovich, D. Veksler, G. Bazalitski, S. Gleizer, A. Grinenko, and V. I. Oreshkin, Plasma Sources Sci. Technol. **19**, 034020 (2010).